

# Measurement of Proton-Induced Nuclear Reactions on Natural Titanium in the High Energy Protons.

M.H. Jung<sup>a</sup>, W.J. Cho<sup>a\*</sup>, H.M. Jang<sup>a</sup>, Y.M. Kim<sup>a</sup>, G.I. Jung<sup>a</sup>, J.K. Park<sup>a</sup>, S.C. Yang<sup>b</sup>

<sup>a</sup>Particle Beam Research Division, Korea Atomic Energy Research Institute, Gyeongju, 38180, Republic of Korea

<sup>a</sup>Nuclear Data Center, Korea Atomic Energy Research Institute, Daejeon, 34057, Republic of Korea

\*Corresponding author: wonje59@kaeri.re.kr

**\*Keywords :** High energy proton, Proton-induced reaction, Titanium

## 1. Introduction

High-energy protons collided with titanium-aluminum stacked targets to measure proton-induced nuclear reactions on natural titanium in the 60-100 MeV energy range. Subsequently, gamma-ray spectra were measured and analyzed using an HPGe detector to calculate the nuclear reaction cross-sections for various radionuclides such as <sup>48,51</sup>Cr, <sup>48</sup>V, <sup>43,44m,46,47,48</sup>Sc, and <sup>43</sup>K originating from titanium. Existing literature predominantly needs more data on nuclear reaction cross-sections beyond 70 MeV, highlighting significant gaps in this energy range. The measured data in this study exhibited good agreement with existing literature, indicating promising prospects for providing new data above 60 MeV.

## 2. Materials and Methods

### 2.1 Proton Beam Irradiation

For proton beam irradiation, the typical stack foils-target was arranged in sets, each consisting of <sup>27</sup>Al foils for beam monitoring, natural Ti and V foils, and 1 or 2 sheets of energy degrader. The stacked samples were fixed behind the collimator ( $\Phi = 10$  mm) and placed at the proton beam line, as shown in Figure 1. Proton beam irradiation was performed on the stacked foil-pellet target at the Korea Multi-purpose Accelerator Complex (KOMAC) facility using 60 to 100 MeV proton energy.

During irradiation, the linear accelerator was operated for 20 min with a repetition rate of 1 Hz. A multi-layer Faraday cup measured the incident proton beam energy, and the proton beam energies for the individual samples were calculated using the Stopping and Range of Ions in Matter (SRIM) code.

### 2.2 Gamma-ray Spectroscopy

The  $\gamma$ -ray spectrum measurements of activated samples were conducted after a sufficient cooling time of 40 h. The  $\gamma$ -ray spectra were measured twice based on the half-life of the radionuclides. All samples were measured with a p-type coaxial high-purity germanium (HPGe) detector and a PC-based 8k channel analyzer.

The energy resolution and relative efficiency of the HPGe detector were 0.875 keV FWHM at 122 keV and 30%. A pileup effect was prevented by keeping the samples placed at 10 or 5 cm from the detector surface and ensuring that the dead time remained less than 5%. For energy and efficiency calibration of the HPGe detector, several certified reference materials (<sup>241</sup>Am, <sup>152</sup>Eu, <sup>137</sup>Cs) were used. Genie-2000 software was used to analyze the  $\gamma$ -ray spectra. A typical  $\gamma$ -ray spectrum of an activated <sup>nat</sup>Ti sample using an HPGe detector is shown in Figure 2.

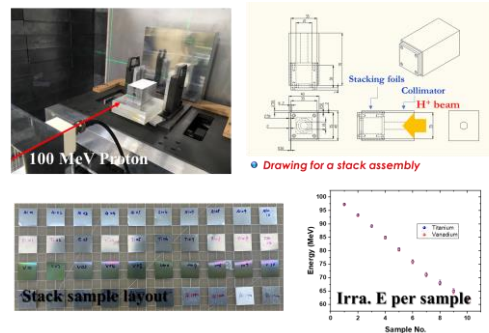


Fig. 1. Experimental setup for proton beam irradiation on target assembly.

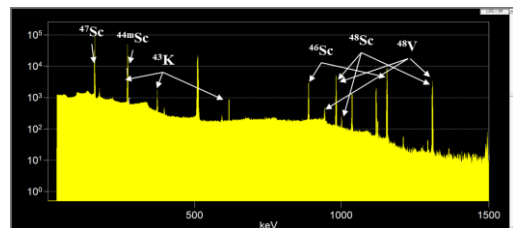


Fig. 2. Typical spectrum of the activated <sup>nat</sup>Ti

## 3. Results and Discussion

After irradiation, all foils were measured using the HPGe system. The cross-sections for <sup>43</sup>K, <sup>44m,46,47,48</sup>Sc, and <sup>48</sup>V were measured for (p,x) reactions in <sup>nat</sup>Ti foils up to 97 MeV, presented in Table 1. The measured cross-sections were compared to the TENDL database and literature.

Fig. 2. Measured cross-sections of the <sup>nat</sup>Ti(p,x) reactions

Energy [MeV]	$^{43}\text{K}$ [mb]	$^{44\text{m}}\text{Sc}$ [mb]	$^{46}\text{Sc}$ [mb]	$^{47}\text{Sc}$ [mb]	$^{48}\text{Sc}$ [mb]	$^{48}\text{V}$ [mb]
97.22±0.08	1.91±0.23	19.24±2.24	44.94±5.19	24.54±1.63	2.50±0.29	14.59±1.81
93.26±0.27	1.77±0.23	18.74±2.19	42.15±4.93	23.11±1.55	2.50±0.29	16.47±2.56
89.16±0.38	1.78±0.24	20.61±2.41	46.57±5.46	24.96±1.68	2.53±0.31	14.36±2.25
84.90±0.47	2.02±0.27	22.01±2.58	48.13±5.67	25.70±1.75	2.66±0.32	17.00±2.67
80.49±0.56	1.53±0.22	21.84±2.56	47.33±5.57	24.29±1.65	2.43±0.30	14.65±2.36
75.89±0.62	1.34±0.20	23.51±2.79	52.16±6.20	25.47±1.79	2.65±0.33	14.74±2.57
71.08±0.69	1.35±0.20	22.85±2.71	48.45±5.77	24.64±1.73	2.42±0.30	14.13±2.42
68.04±0.87	1.14±0.18	21.81±2.66	48.80±5.98	24.06±1.82	2.39±0.30	13.58±2.42
64.92±0.77	1.37±0.21	21.05±2.54	51.48±6.24	24.29±1.80	2.29±0.29	14.19±2.38
61.69±0.84	1.56±0.23	19.58±2.37	51.81±6.30	25.11±1.87	2.25±0.29	3.02±16.17

### 3.1 Production of $^{43}\text{K}$

This work presents results similar to those of other literature in Figure 3. A well-matching excitation function is obtained that corresponds well with values proposed by M.B. Fox et al.

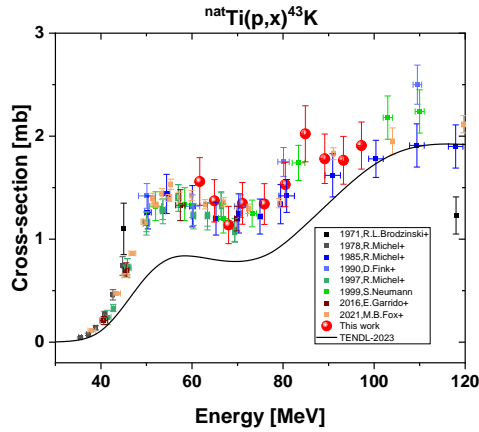


Fig. 3. Cross-section for the production  $^{43}\text{K}$  via the  $^{\text{nat}}\text{Ti}(p,x)$  reaction

### 3.2 Production of $^{44\text{m}},^{46},^{47},^{48}\text{Sc}$

This work is consistent with all prior data but generally shows values slightly higher than the previous data. Those data are plotted in Figures 4 to 8.

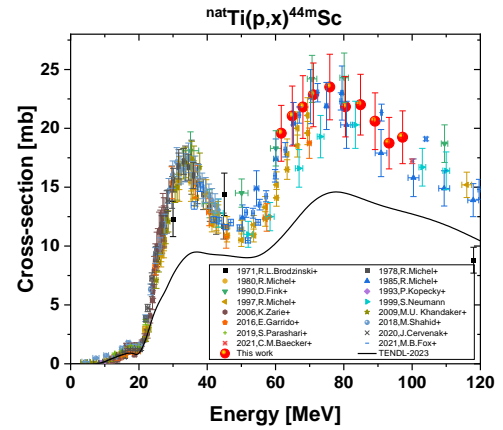


Fig. 4. Cross-section for the  $^{\text{nat}}\text{Ti}(p,x)^{44\text{m}}\text{Sc}$  reaction

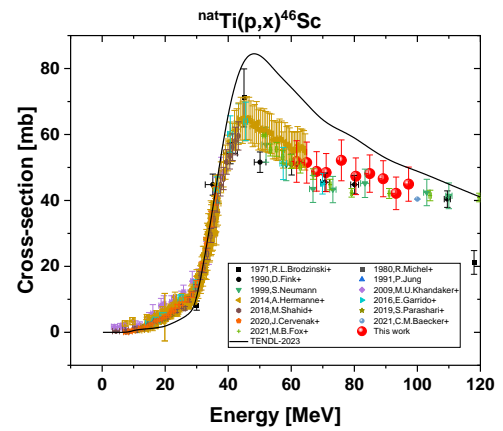


Fig. 5. Cross-section for the  $^{\text{nat}}\text{Ti}(p,x)^{46}\text{Sc}$  reaction

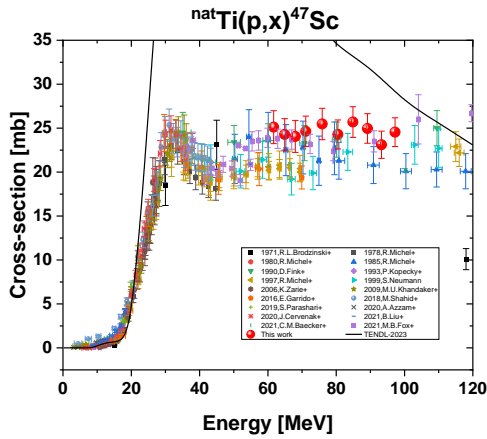


Fig. 7. Cross-section for the  $^{nat}\text{Ti}(p,x)^{47}\text{Sc}$  reaction

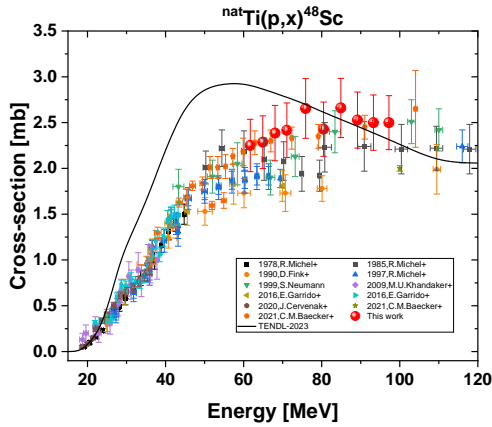


Fig. 8. Cross-section for the  $^{nat}\text{Ti}(p,x)^{48}\text{Sc}$  reaction

### 3.3 Production of $^{48}\text{V}$

This reaction channel is used to monitor the beam current of the protons. There is so much previous literature. This work shows (Figure. 9) upwardly shifted values when compared to other literature.

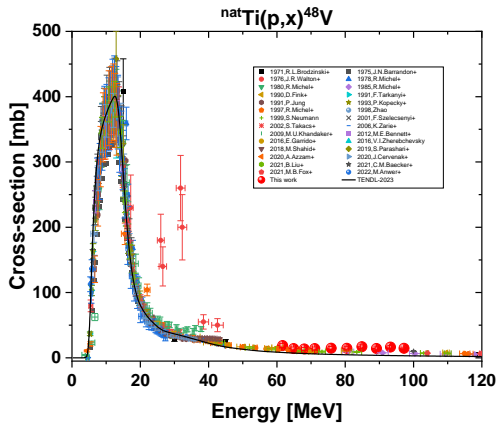


Fig. 9. Cross-section for the  $^{nat}\text{Ti}(p,x)^{48}\text{V}$  reaction

In this study, we present new measurements of excitation functions for the  $^{nat}\text{Ti}(p,x)^{43}\text{K}$ ,  $^{44\text{m},46,47,48}\text{Sc}$ , and  $^{48}\text{V}$  reactions in the energy range 61–97 MeV. Our cross-sections were compared with previously published experimental data and with prediction of the nuclear reaction model code TALYS adopted from the TENDL-2023 online library. The data shown in this study generally tend to show higher values of nuclear reaction cross-sections compared to the other literature. Slight differences can be due to errors in the beam current measurement or in the detector efficiency calibration. We plan to carefully review this issue.

## REFERENCES

- [1] J.F. Ziegler, J.P. Biersack, M.D. Ziegler, SRIM, the Stopping and Range of Ions in Matter, SRIM Company 2008
- [2] N. Otuka, E. Dupont, V. Semkova, B. Pritychenko, A.I. Blokhin, M. Aikawa, S. Babykina, M. Bossant, G. Chen, S. Dunaeva, R.A. Forrest, T. Fukahori, N. Furutachi, S. Ganesan, Z. Ge, O.O. Gritzay, M. Herman, S. Hlavač, K. Katō, B. Lalremruata, Y.O. Lee, A. Makinaga, K. Matsumoto, M. Mikhaylyukova, G. Pikulina, V.G. Pronyaev, A. Saxena, O. Schwerer, S.P. Simakov, N. Soppera, R. Suzuki, S. Takács, X. Tao, S. Taova, F. Tárkányi, V.V. Varlamov, J. Wang, S.C. Yang, V. Zerkov, Y. Zhuang, Towards a More Complete and Accurate Experimental Nuclear Reaction Data Library (EXFOR): International Collaboration Between Nuclear Reaction Data Centres (NRDC), Nuclear Data Sheets, 120 (2014) 272-276.
- [3] F.T. S.M. Qaim, R. Capote, Nuclear Data for the Production of Therapeutic Radionuclides, Technical Reports Series No. 473, International Atomic Energy Agency, 2011.